Conference Proceedings

EuroSun 2016
Palma de Mallorca (Spain), 11 - 14 October 2016

Using detailed TRNSYS models for fault detection in solar domestic hot water systems – a case study

Simon Maltais Larouche and Michaël Kummert

Polytechnique Montréal, Dept. of Mechanical Engineering, Montréal (Québec), Canada

Abstract

This paper describes the application of TRNSYS simulations for Automatic Fault Detection (AFD) in a medium-size (35.5 m²) Solar Domestic Hot Water (SDHW) system located in Montréal, Québec, Canada. The system was designed by students in 2011 and was equipped with a detailed monitoring system, which provided the opportunity to develop and validate a fault detection methodology using detailed simulation. The paper presents a two-level automatic fault detection method combining a rule-based algorithm and TRNSYS simulations. The two methods show strengths in detecting different types of faults, but also a sensitivity to false alarms. Using both methods combines their detection capabilities but also increases the AFD robustness against false alarms. It can help diagnose the cause of the detected faults and, when integrated in a effective user interface, it can contribute to increase the reliability of SDHW systems.

Keywords: *solar domestic hot water, fault detection, solar energy, simulation, modeling, TRNSYS*

1. Introduction

The 2011 annual meeting of the American Society for Heating, Refrigerating and Air-Conditioning Engineers (ASHRAE) took place in Montréal, Québec, Canada. At that occasion, ASHRAE donated 20,000 $ for a "sustainable project" to be implemented in the host city. The Montréal chapter of the Society selected a project proposed by a group of students and a local engineering firm to design and install a Solar Domestic Hot Water (SDHW) system for a charity that serves meals to the homeless. The charity, known as Accueil Bonneau, serves more than 800 meals per day and uses a large amount of hot water for dishwashing.



Figure 1: Solar collectors

The system was designed by students within a final year "capstone" project using TRNSYS simulations, between September 2010 and May 2011. It was built during the 2011 summer, and has been delivering close to 45 % of the hot water demand since then (this includes a contribution by a grey water heat recovery system also proposed and designed by the students). Student involvement is continuing through the development of an online monitoring and fault detection system.

The main objective of this paper is to describe the development and results of an Automatic Fault Detection (AFD) system that was implemented on this solar thermal system. The AFD system is based on simple rules and on detailed TRNSYS simulations.

The paper starts with an overview of the system design and instrumentation (section 2), which is followed by a brief presentation of the historical performance and its comparison with the original design simulations (section 3). Although the long-term performance seems satisfactory, the monitoring results show signs of potential underperformance and several system faults were recorded. Section 4 presents a brief literature review and a description of the AFD algorithm. The results of the proposed method are presented in section 5, which leads to the discussion and conclusions.

2. System design and instrumentation

The system design was influenced by severe space constraints in the mechanical room and on the roof. A large part of the roof is affected by local shading by a church tower in the South South-West direction. The building is also located in a historical heritage site (Old Port of Montréal), so the collectors had to be concealed from direct view from the street. This resulted in a suboptimal orientation for the collectors, which are facing East South-East (110° East from North) with a slope of 39°. The project objectives called for a zero-cost for the end-user (the Accueil Bonneau charity), so component selection was also affected by opportunities to involve partners who were willing to contribute equipment at no-cost or very low cost. The selected collectors are 11 modules of Kingspan Thermomax HP200-30, which are heat-pipe evacuated tubes with 30 tubes and a 3.23 m² aperture area per module. The modules are connected in a series-parallel layout with 3 parallel branches of 3 modules in series (one branch of 2).

The system schematic shown in Figure 2 shows a classical closed-loop preheating Solar Domestic Hot Water (SDHW) configuration. The glycol loop with the solar collector transfers heat through coil heat exchangers located in the preheat tank. The DHW is then heated in an auxiliary tank, which is fed by a gas boiler. A thermostatic valve ensures that the distributed DHW does not exceed the desired temperature, even in the case of high temperature in the solar tank. Because of space constraints and cost, the preheat tank consists of three 120-USgal (450 L). Design simulations compared series and parallel configurations and concluded that the series configuration offered the best performance, in addition to simplifying the hydronic network design and balancing. The controller is a classical model (Caleffi iSolar Plus), which measures the temperature at the solar collector outlet and at the bottom of the (coldest) solar tank to activate the pump (see Figure 2).

The existing gas water heater was not modified, and it acts as the auxiliary heat source for the SDHW system. It consists of a gas boiler and a buffer tank that includes a coil heat exchanger for the DHW (Thermo2000 Turbomax tank, which includes multiple copper coils in parallel). The system includes a Grey Water Heat Recovery (GWHR) heat exchanger (the mains water goes through a coil wrapped around the main drain pipe).

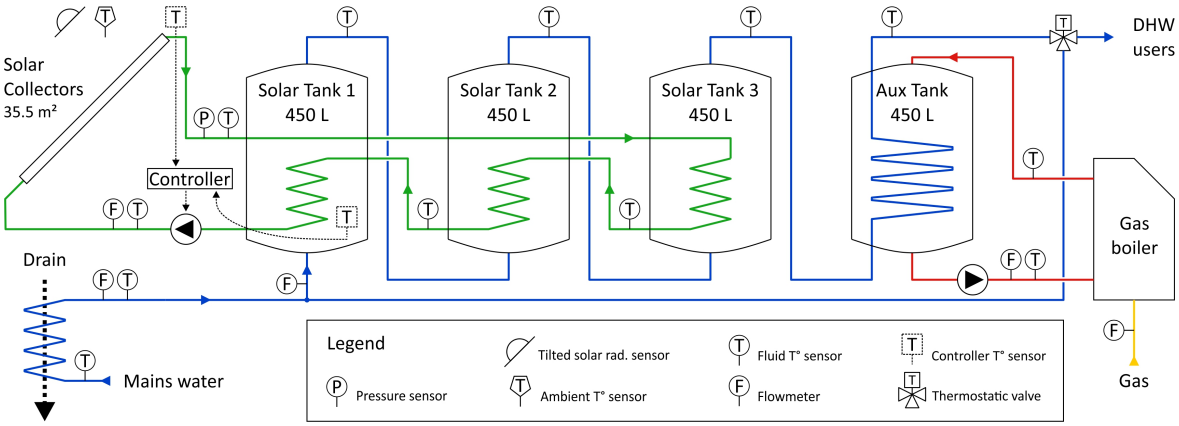


Figure 2: System schematic with installed sensors

In line with the educational objectives of the project, a detailed monitoring system was installed to allow the next cohorts of students to assess the performance of the system and learn from the real operating data. Figure 2 shows the location of the main sensors. The data acquisition system monitors the ambient conditions (tilted solar radiation in the collector plane and air temperature), the DHW temperature in 8 locations, the glycol loop temperature in 4 locations, the boiler loop temperature in 2 locations, the DHW flowrate (total and through the solar tanks), the glycol flowrate, the boiler loop flowrate, and the gas consumption.

The system was designed based on an estimate of the domestic hot water use of 4715 L/day, which was extrapolated from 2-week records. The supply temperature at the time was assumed to be 55 °C, which is not consistent with the current thermostatic valve setting. It is unclear whether the setting was changed or whether the design assumption was wrong. The design simulations estimated the energy demand for DHW at 310 GJ/year, with a net contribution of 20 % for the GWHR and 30 % for the solar system (see next section).

3. Historical system performance

Operational data are available since 2012 with a 1-minute sampling rate, with some missing data in 2014 due a failure and the replacement of the data logger. Figure 3 shows the overall energy balance of the system based on available data, expressed in annual values. The results show that the net energy demand for DHW (230 GJ) is significantly lower than expected, and corresponds to an average DHW use of 4465 L/day at an average temperature of 46 °C after the thermostatic valve. The GWHR contributes 20 % of that net energy demand, and the solar system contributes 24 %. The average solar collector net thermal efficiency is 35.5 % (accounting for solar collectors, piping, and solar tanks losses).

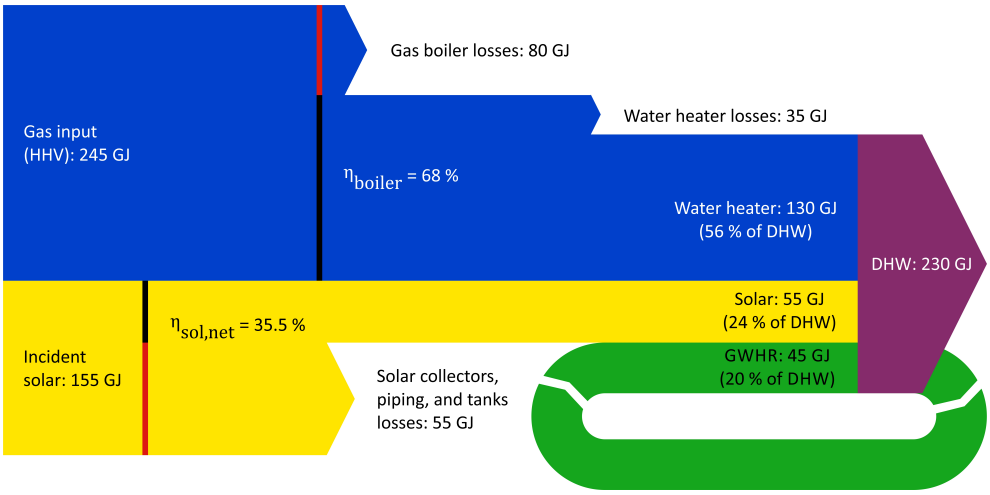


Figure 3: Sankey diagram of the annual system performance

The annual gas consumption amounts to 6500 m³ (the Higher Heating Value, HHV, is 37.5 GJ/m³). Assuming constant water heater losses and a constant boiler efficiency, the gas consumption of a reference system (without GWHR nor solar thermal) can be calculated as 10500 m³. The savings amount to 4000 m³ of gas annually, which corresponds to avoided emissions of 7.5 tonnes of CO_2 per year. The solar thermal contribution is lower than estimated in the design simulations, but such an annual energy balance cannot identify the cause for the system underperformance (or confirm that the system operation is normal while the design simulations were wrong). Figure 4 shows the monthly contributions to the net DHW demand.

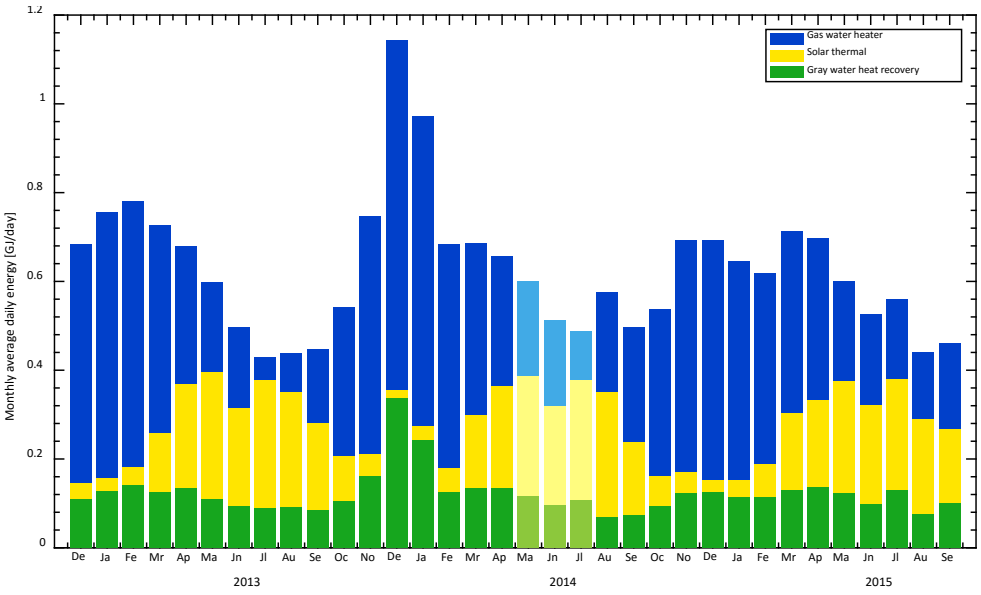


Figure 4: Monthly performance of the system (light colored bars are estimated)

As expected, the solar thermal contribution is higher in summer and lower in winter. The variation of the DHW load with the season (due to colder mains water in later winter and spring) is exacerbated by the variability of the DHW volume used by the charity. The DHW volume shows a general trend with higher values in winter (with more meals served to homeless people), some months show unexpectedly low or high

usage (between 3500 L/day and 6500 L/day for the monthly average, or between 80 % and 145 % of the long-term average).

Figure 5 shows the daily incident solar irradiation on the collector array, and the net solar thermal output. The figure illustrates the difficulty of obtaining quality long-term data on a system's performance, with a large number of missing days in 2014. The first data acquisition system was a relatively old system obtained free of charge from one of the project partners, and it failed after 1.5 years of service. The graph shows some days in winter with a relatively large incident radiation but very little or no solar thermal output.

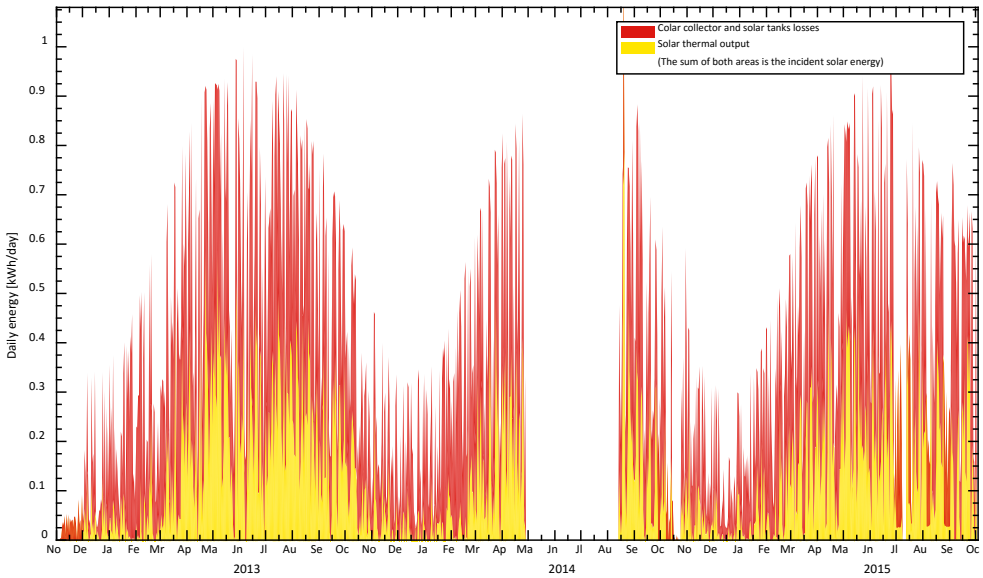


Figure 5: Daily solar incident irradiation and net solar thermal output

Figure 6 shows the daily net solar thermal efficiency. It highlights strong differences in day-to-day system efficiency, with values up to 150 % (not shown in the graph, trimmed at 100 %) and negative values.

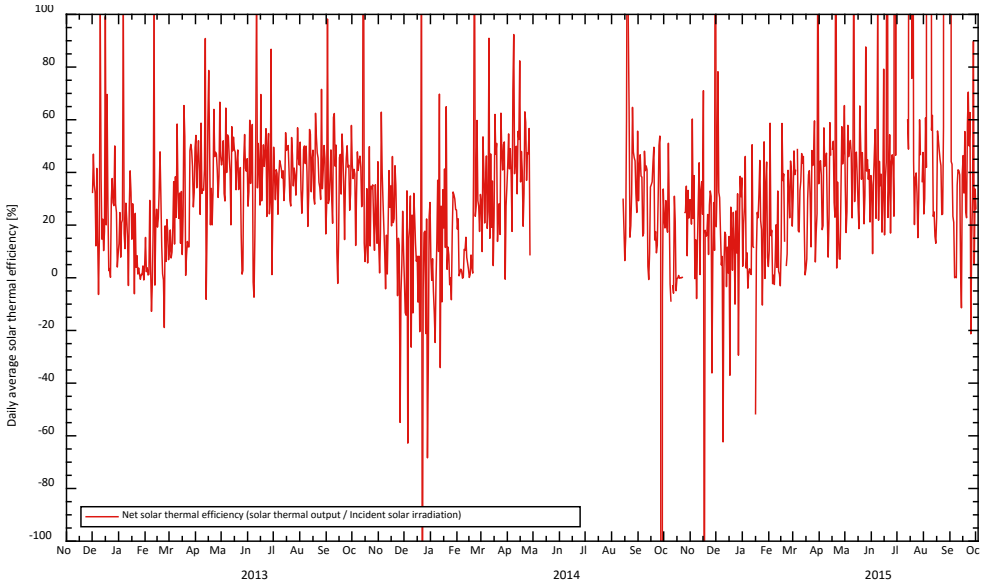


Figure 6: Daily net solar efficiency

These values point at potential problems in the system operation, although the system operator reported no problem or failure during the whole period, apart from a failure of the auxiliary gas boiler and a major leak incident in the solar thermal tanks (a plug installed in an unused connection port had been incorrectly selected, corroded, and failed).

A detailed analysis of the system behavior allowed to identify a few issues related to the pump operation and the system performance during very cold days. This led to the development of an Automatic Fault Detection algorithm, which is described in the next section.

4. Automatic Fault Detection algorithm

4.1. Literature review

Reliability studies show that faults are frequently encountered on many SDHW systems due to poor design, careless installation, poor control strategies, inadequate maintenance, etc. As an example, (Menicucci, 2009) shows that about 50 % of 71 SDHW systems installed in the USA in the 90's were experiencing serious issues after 10 years of operation and the majority of these failing systems where not operating at all.

A solution to increase SDHW systems reliability is to allow early fault detection through automatic fault detection strategies. A detailed overview of the long-term FD methods that were developed for STS in recent years is presented by de Keizer et al. (2011a). The methods are compared via a multi-criteria analysis which includes a comparison of the accuracy, cost, state of development and other criteria. Their summary shows that most of the presented methods are still at a research stage and that little data is available on practical implementations. To the authors' knowledge, the only method that was commercialized is the so-called "input-output" controller (Pärisch and Vanoli, 2007).

A frequently encountered method consists in verifying that the monitored variables (e.g. solar tank temperature) do not exceed acceptable thresholds through the application of rule-based algorithms, as proposed among others by (Holter et al., 2011) and (Küthe et al., 2011). This solution is relatively easy to implement since it only requires information on the system's expected normal operating conditions. Rule-based algorithms are well suited for the detection of abrupt changes in operating conditions and relatively easy to program and implement. A major drawback is that they are less sensitive to slowly occurring faults such as heat exchanger fouling.

Applications of self-learning, data-driven algorithms such as Artificial Neural Networks (ANN) are also found in the literature (He et al., 2012; Kalogirou et al., 2008; Yaïci and Entchev, 2014). ANNs act like black-box models and do not require *a priori* knowledge of the SDHW system. Instead, an ANN learns to establish relationships between inputs (e.g. collector inlet temperature, global solar radiation, etc.) and an output (e.g. collector outlet temperature) through a learning process. The learning process uses data generated by a (physics-based) simulation program such as TRNSYS (Klein et al., 2014) or historical recorded data. An ANN based FD system should trigger an alarm if the measured output is significantly different from its predictions. The advantages of ANN are that they easily deal with noisy or incomplete data which could cause problems with standard rule-based algorithms. However, an inaccurate or insufficient training could lead to many false alarms since the ANN would make inaccurate performance predictions.

A different approach is presented by de Keizer et al. (2013), which is based on an energy simulation tool (TRNSYS) to assess the solar circuit and auxiliary heating device performance. The simulation results are then compared with on-site measurements. Two symptoms: *too low solar energy yield* and *too much auxiliary heating* are generated if abnormal conditions are encountered. Comparisons were performed between simulation results for the daily energy and measurement from existing field SDHW systems of multiple sizes and configurations. Depending on the uncertainty margins on simulation results and measurements, an energy loss of more than 25 % was identifiable. It was also recommended to use this method in combination with standard rule-based algorithms because they are more suitable for system control monitoring and fault isolation.

The proposed method described in this paper uses a combination of a rule-based algorithm and a simulation-based algorithm. The AFD methodology is applied to actual data from the system described in the previous sections.

4.2. Proposed architecture

The proposed AFD strategy is part of a complete framework organized in four layers as shown in Figure 7. The first two layers perform data management, including data acquisition and storage of measurements and fault events in a database. The third layer consists of two levels of FD. Level 1 is based on an algorithm that performs standard rule-based FD every 15 minutes. Then a system performance assessment against daily performance simulation is done into the second layer. Once a day, the energy yield of the solar array and the auxiliary heating device energy use are calculated from measurements and are then compared with the predictions of a simulation model, with the objective of identifying significant differences. The fourth layer is only activated if one or more faults are detected. The user is notified through a user interface and by direct messages (e.g. by email) if abnormal conditions are identified. More details on the methodology are available in the First author's Master thesis (Maltais Larouche, 2016).

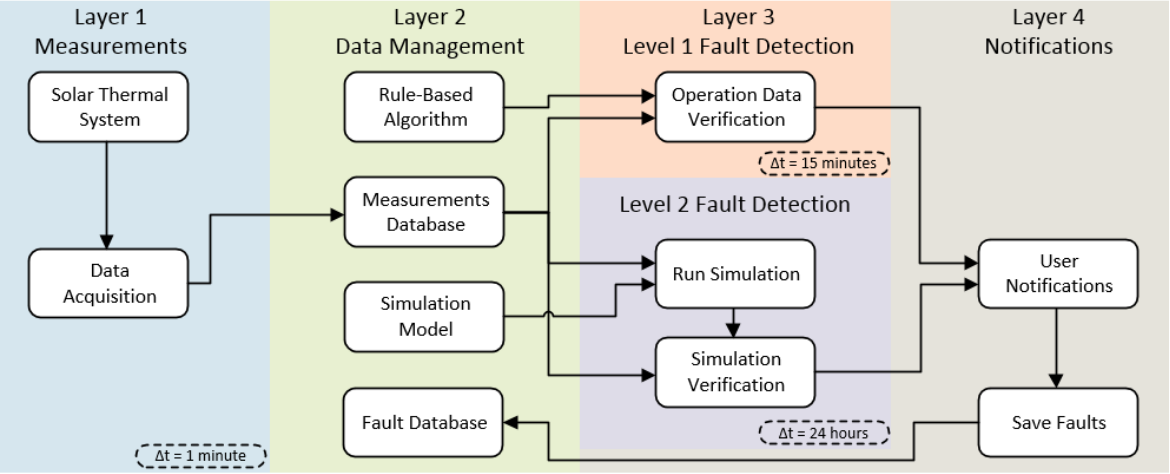


Figure 7: Layout of the proposed fault detection algorithm

Level 1: rule-based fault detection

The first fault detection level is composed of a set of rules, from simple thresholds to more complex rules such as plausibility checks. Table 1 shows an excerpt of the rules that are being verified when a performance analysis is required by the monitoring framework. As an example, the second rule on Table 1 triggers a fault signal if no flowrate is measured in the last 24 hours, which would be very unlikely for this system. That rule also illustrates the fact that, even though rules are checked every 15 minutes, they do not necessarily refer to 15-min values, as they can use a longer-term history of key variables (24 h in this particular case). Fault detection occurs if the monitoring data does not comply with one or more of the rules, and a notification is sent to the system owner.

Table 1: Excerpt from the first level fault detection rules

Description	Example of fault detection rule
Basic verification of the measurements (Temperatures, flowrates, pressure, etc.)	$T(t) < T_{min} \ OR \ T(t) > T_{max}$
No DHW flowrate in the last 24 hours period	$\sum[Flowrate(t)] = 0$
Flowrate in the solar circuit at night	$Circuit\ Flow(t) > 0 \ AND \ [t < t_{sunrise} \ OR \ t > t_{sunset}]$
Solar radiation is measured at night	$G_{tilted}(t) > 25\frac{W}{m^2} \ AND \ [t < t_{sunrise} \ OR \ t > t_{sunset}]$
Logical comparison in order to detect inconsistencies between two or more measurements	$T_{Aux,in} > T_{Aux,out} + 5℃ \ AND \ Auxiliary \ Heating = ON$
Impossible measurements (e.g. unconnected sensor, data acquisition wrong configuration, etc.)	$T(t) < T_{Impossible,min} \ OR \ T(t) > T_{Impossible,max}$

Level 2: Simulation based fault detection and simulation models

The second level of fault detection consists of daily numerical simulations of the system performance. They aim at obtaining an estimate of the solar yield and the auxiliary heater output using "actual" on-site data for environmental conditions (solar radiation and temperature and DHW demand. A fault signal is then triggered if the measured energy quantities are considered to be significantly different from the simulation results.

Figure 8. shows an overview of the detailed TRNSYS model which is used in the fault-detection algorithm. Most of the components in the simulation (known as TRNSYS "Types") are standard TRNSYS or TESS models (Klein et al., 2014; Thornton et al., 2013) except for Type 3911 which is a variable flow controller developed by the authors to reproduce the behavior of the installed controller. Simulations are performed using a 1-min time step to match the measured data sampling time. A "warm-up" period of 48 h is simulated using historical data before the new 24-h period is simulated, in order to get correct initial conditions for the solar thermal tanks and other components with thermal mass in the simulation.

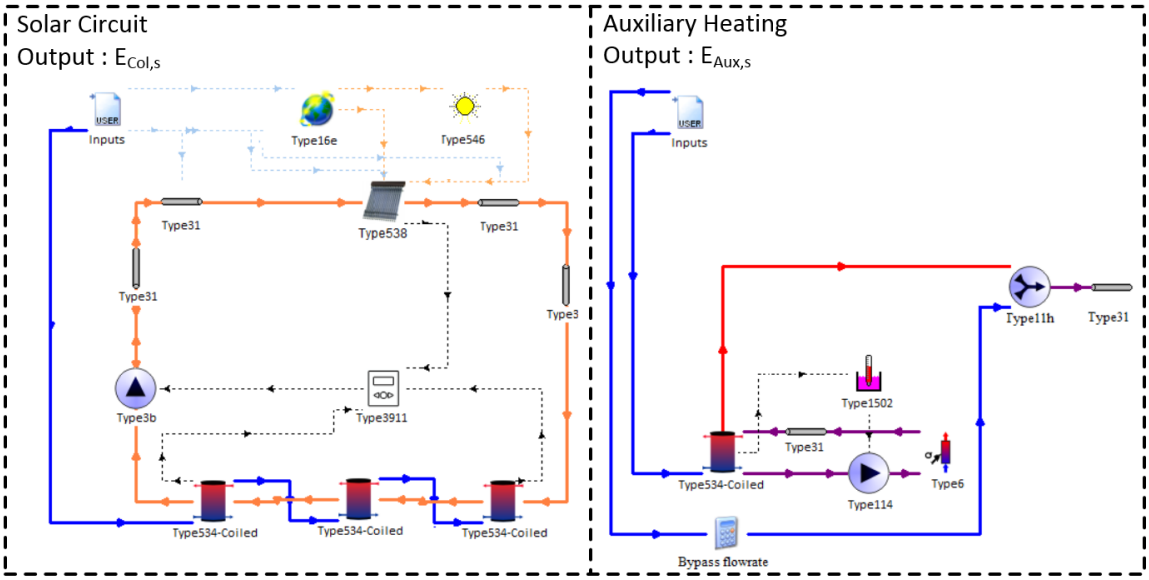


Figure 8 : TRNSYS model used for fault-detection (2 sub-models, solar circuit and auxiliary heating)

It is important to note that the TRNSYS model effectively consists of two independent sub-models (*Solar Circuit* and *Auxiliary heating*). The solar tanks DHW output is not directly linked to the auxiliary heater tank. Instead, the outputs from the first subsystem (solar circuit) are used to perform fault detection on the solar thermal system, and inlet conditions for the auxiliary heater are read from a file populated with measured values. This helps isolate the origin of a potential fault, instead of propagating the fault (or simulation error) impact from one subsystem to the other.

The TRNSYS model employed in this paper is calibrated using on-site data, and it uses on-site measured solar radiation and temperature data. A further analysis of the differences with an un-calibrated model and with a model using web-based weather data is presented in (Maltais Larouche, 2016).

User interface

The limited expert knowledge on solar systems and the lack of time to monitor and analyze systems were often identified in the literature as causes for undetected or uncorrected faults. It is therefore important to provide an easy to understand user interface which allow systems owners to be quickly informed of abnormal operating conditions. When faults are detected, the system operator should be able to know the nature, the location and the severity of these events in a visual and simple manner. Figure 9 shows an example of how the outcomes of the proposed methodology were presented. The fault location(s) is(are) identified a simplified system layout and supplementary information about the faults are displayed on the right side graph. Fault type, severity and time of occurrence are clearly indicated to help system operators in decision making.

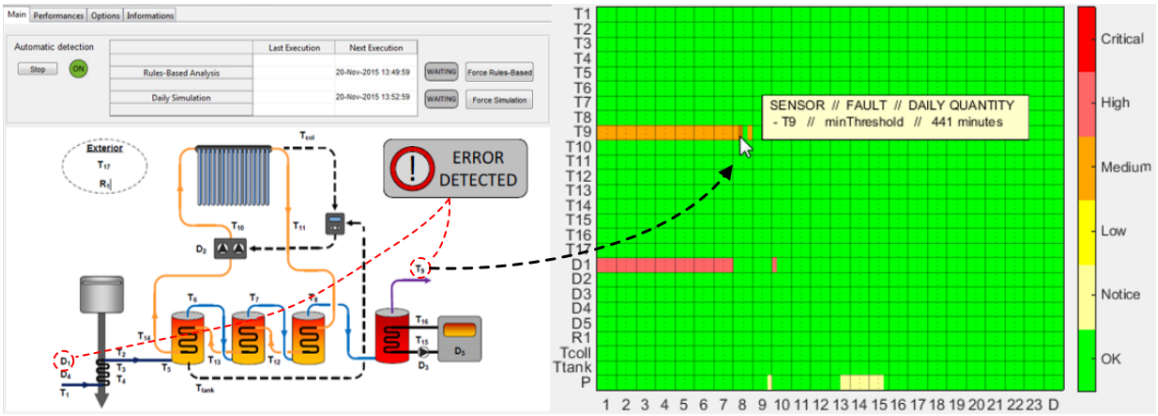


Figure 9 : Example of user interface display with daily results

5. Results

An assessment of the Automatic Fault Detection (AFD) method was completed using monitoring data of 650 days from 2013 to 2015. The results obtained from the analysis are displayed on Figure 10. Fault detections obtained from the rule-based algorithm and simulation are displayed respectively on the bottom and upper carpet plots were the color mapping indicates the severity that has been assigned by the algorithm to a particular fault (see color bar on the right).

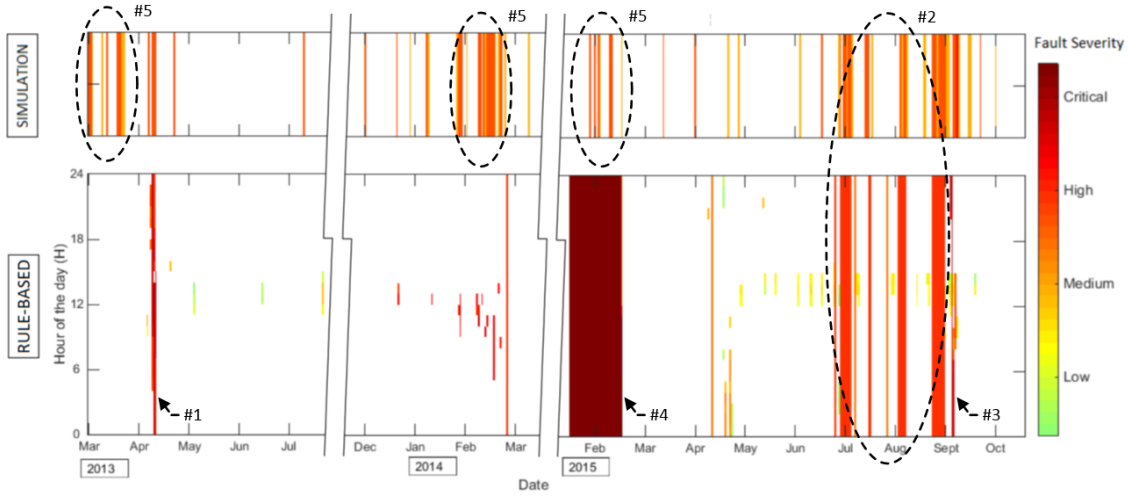


Figure 10 : Global result presentation

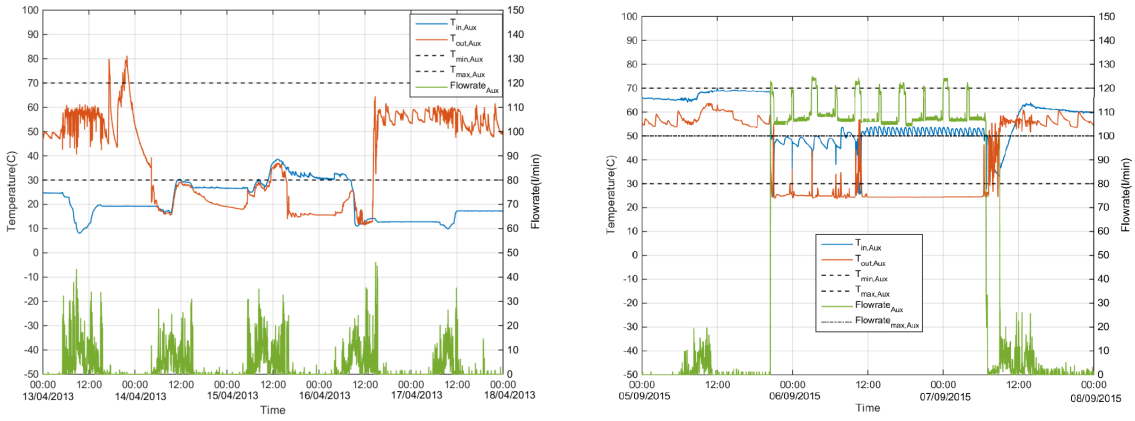
A first look at Figure 10 shows that many faults were detected by the rule-based method as well as the simulation-based method over the assessed period. Faults were sometimes detected simultaneously by the two methods, but not always. As an example, many faults were identified by the simulations in March 2013 but none were by the rule-based algorithm. False detection is a common problem in AFD algorithms, which sometimes represents a significant annoyance for system operators and leads to the AFD system being ignored or disabled. The following sections examine the detected faults in detail and discuss the implications on the proposed 2-layer method.

5.1. Fault detection by the rule-based algorithm

As shown in Figure 10, multiples faults were detected by the rule-based algorithm with different time patterns and severity levels. The period between March 2013 and early 2014 was almost exempt of faults, apart from one event in April 2013 [#1 in Figure 10] which was generated by the auxiliary heater failure (see below). In contrast, multiple detections are visible from February to October 2015 [#2, #3 and # 4]. Most of the detections [#3 and #4] were determined to be related to instrumentation problems, while one event was related to a failure of one of the solar tank.

The rule-based algorithm detected abnormal system conditions brought by two major system failures that occurred in April 2013 [#1] and September 2015 [#3]. The first fault event is related to a failure of the gas boiler feeding the auxiliary heater, which led to abnormal flow and temperature condition (the gas boiler was subsequently replaced). The measured inlet and outlet tank temperatures and tank flowrate during this event are displayed of Figure 11 a). The auxiliary heater outlet temperature went over the allowed maximum (70 °C) and then dropped to a value very close to the mains water temperature, indicating no auxiliary heat during the April 13/14 night. Afterwards the temperature went below the permitted minimum temperature, since the boiler was not working anymore. The exceeded thresholds have led to multiple fault detections from April 13th to April 16th. Interestingly, this fault was quickly detected by system operators, even though the AFD system was not in place at the time. The auxiliary heater failure had a direct impact on user comfort (cold water instead of hot water), so the problem was quickly detected and quickly remedied.

The second “real” fault event happened on September 5th, 2015. A plug installed in an unused connection port of one of the solar tanks had been incorrectly selected, corroded, and failed. This caused a major leak from the solar storage tanks, which partially flooded the mechanical room. Figure 11 b) shows the operation data that were monitored during this event. The flowrate through the tanks was abnormally high, and exceeded the predefined thresholds, leading to a fault being triggered. Again, the AFD system was not in place at the time, and the monitoring data show that it took almost three days for the system owner to detect the problem, since hot water was still available through the auxiliary heater.



a) b)

Figure 11 : System operation conditions during fault detection events. a) Failure of the auxiliairy heater, b) failure of a solar tank.

Figure 10 shows that the fault event related to the solar tank failure, which is labeled #3, is buried in a succession of faults that started in July 2015 and that are related to instrumentation problems. As an example, faults were detected due to periodic erroneous and noisy solar radiation measurements [#2] as shown in Figure 12.

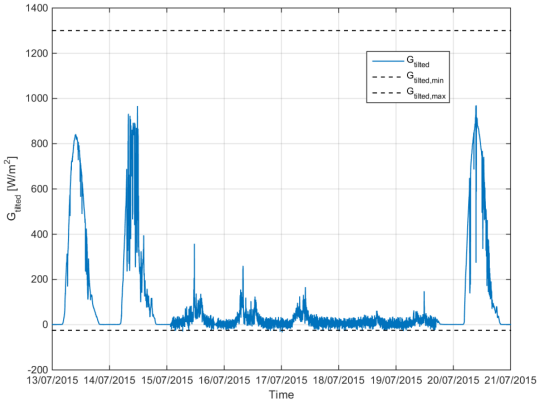


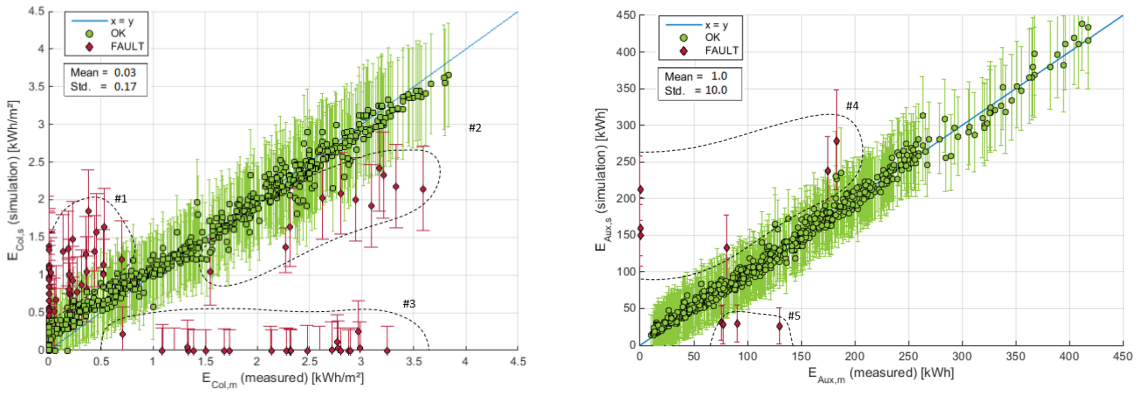
Figure 12 : Failure of the solar radiation sensor

The relatively long period with "critical" failure in February 2015 [#4 in Figure 10] is also related to instrumentation problems rather than to real system faults – the solar circuit pressure sensor was disconnected.

The examples above show that many faults detected by the rule-based algorithm do not indicate problems with the system, but they rather indicate malfunctions in the instruments put in place to monitor performance and detect faults. While it is reassuring to see that the rule-based fault detection would have triggered a major ("high") fault event during the mechanical room flooding, it is unclear whether the system operators would have taken action more quickly, given the numerous false alarms that would have occurred over the previous months. This illustrates the need for simple and reliable data acquisition systems, but also possibly the need to use different algorithms to improve the AFD robustness against false alarms. The next section shows how the approach based on detailed TRNSYS simulations can help achieve that objective.

5.3. Fault detection using TRNSYS simulations

The daily comparison between simulation and measurement have brought to the identification of about 99 faults, which are shown in the top part of Figure 10, above. From these, 89 faults were related to the solar circuit and 10 to the auxiliary heater. The results are presented on Figure 13, where the x-axis shows the measured daily energy and the y-axis shows the simulation prediction. Faults are identified by red diamonds. Scatter plots for the collector output and auxiliary heat are aligned with the x = y line with a relatively small standard deviation, and the uncertainty on simulated results is acceptable (more information on how the uncertainty is estimated can be found in Maltais Larouche, 2016).



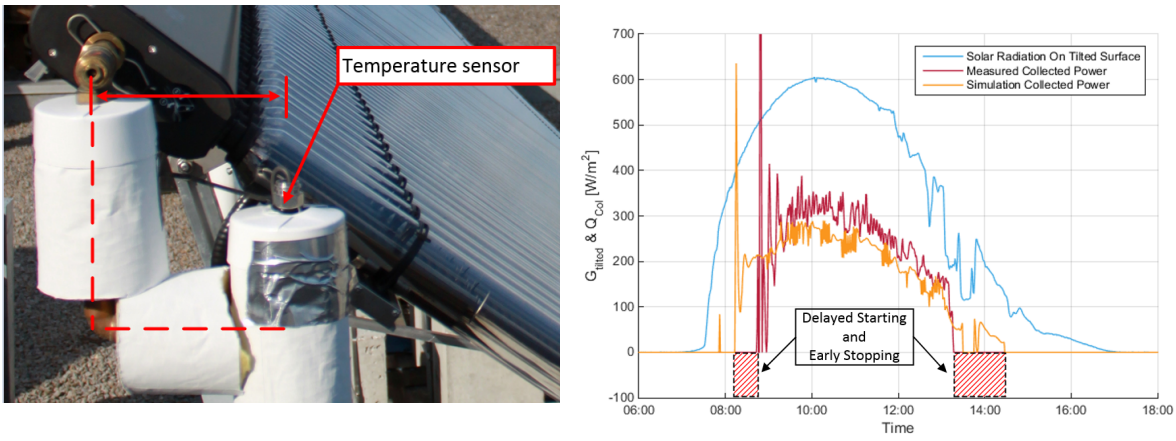
a) Solar circuit **b) Auxiliary heater**

Figure 13 : Simulation-based fault detection method – results overview

An in-depth analysis of the identified faults for the solar circuit shows that the results can be divided into three sets, identified in Figure 13 a).

Faults in set #1 were detected on very cold days due to a combination of the following causes:

- During the 2013/14 winter, the concentration of antifreeze (propylene glycol) in the solar loop was insufficient. Ironically, this problem occurred when a plumber refilled the system with water after replacing a flowmeter in the solar circuit in order to improve monitoring and AFD. The insufficient glycol concentration prevented the pump from operating normally at ambient temperatures below -15 °C but did not result in major damage. The glycol concentration was adjusted during the next summer.
- The temperature sensor used by the control system to monitor the collector outlet temperature was installed incorrectly, slightly away from the collectors in the return line. The sensor well was also insufficiently insulated from ambient conditions. This causes delayed start and early stop of the solar circuit pump during most days, resulting in a decreased collected energy. This is illustrated in Figure 14. Unfortunately this problem is frequent in SDHW systems, especially with heat pipe evacuated tube collectors, and some controllers are now equipped with specific operating modes to mitigate this problem (Viessmann, 2015).
- Collectors are sometimes partially or completely covered by accumulated snow. Although Montréal receives over 2 meters of snow over a normal year, this problem is infrequent as snow is normally quickly blown away by wind and partial melting, given the location on a roof and the relatively large space between the collector bottom and the roof surface (about 40 cm).



a) **b)**

Figure 14 : Example of delayed start and early stop due to a badly positioned collector outlet temperature sensor on January 26th 2015.

Unlike the first set of faults, sets [#2] and [#3] do not represent actual system faults but result from erroneous measurements. Faults detected in [#2] correspond to incorrect (overestimated) values from the solar circuit

flowmeter, which result in an overestimation of the measured collected solar energy. Faults from set [#3] were generated by incorrect values of the solar radiation sensor (very low values), which resulted in no useful solar output in the simulation. This highlights the importance of having a reliable data acquisition system and to check the measurements with a rule-based algorithm before launching the simulation since it is more reliable for instrumentation error detection. It also shows the possibility to increase the AFD robustness by using web-based weather data, as discussed in (Maltais Larouche, 2016).

Faults detected in the auxiliary heater subsystem were divided into two sets, [#4] and [#5], as shown on Figure 13b). Set [#4] corresponds to a failure and replacement of the auxiliary gas boiler, and to 3 occasional maintenance events when the gas boiler was off. These events were also identified by the rule based-algorithm. Faults detected in [#5] correspond to the failure of a corroded plug in the solar tanks that was also clearly identified by the rule-based algorithm.

5.3. Combination of rule-based and simulation-based algorithms

The previous results show that both methods are capable of performing fault detection for real operating conditions on a real SDHW system. But missed fault events and false alarms point at some limitations of the individual approaches:

- The rule-based method was not always capable of differentiating between real system faults and instrumentation errors. This led to false alarms or to an incorrect fault severity level (e.g. “critical” failure detected when the pressure sensor was disconnected).
- The rule-based method could not detect slowly occurring faults or faults that have no significant impact on operating conditions relative to predefined thresholds (e.g. badly positioned collector outlet temperature sensor).
- Simulations proved to be very sensitive to instrumentation errors related to input data (e.g. bad solar radiation signal). This resulted in erroneous performance prediction and in some occasions to false alarms. The comparison with measured energy performance also depends on extra sensors that are not critical to the system operation and can fail (e.g. flowmeter in the solar collector loop).

The proposed 2-layer Automatic Fault Detection (AFD) framework combines both methods, which have been shown to complement each other. The rule-based layer is used to detect abnormal values in the monitored data which would result in erroneous simulation results. In the case of weather data, they could then be replaced by web-based data to proceed with the simulations. The rules can also detect conditions in which the uncertainty on simulation results would be too high, indicating that possible faults detected by simulations can be ignored. A typical case would be a very cloudy day with little or no solar thermal output. On the other hand, the simulation can proceed with partial data (e.g. it does not require measured pressure in the solar loop), and it can compare results obtained with local weather measurements to those obtained with web-based data. It then has the potential to confirm that the system is delivering a satisfactory energy output, even when the rule-based algorithm has detected problems. While the simulation-based algorithm cannot “remove” a fault, it can lower the severity of some problems detected by rules if they have no impact on the energy performance. And, as illustrated above, simulation also has the potential to detect faults that would go unnoticed by the rule-based algorithm. The combination of both detection algorithms represents a step towards more efficient fault diagnosis – although this was not implemented in our approach, the “critical fault” detected by rules due to an unconnected pressure sensor could be lowered to a “low” level if the energy performance is satisfactory, and a diagnostic could be inferred (probable problem with the pressure sensor rather than with the actual system pressure).

6. Discussion and conclusions

This paper presents an Automatic Fault Detection (AFD) method for Solar Domestic Hot Water (SDHW) systems based on two levels. The first AFD level consists in running a rule-based algorithm which ensures that on-site measurements comply with pre-established limits and rules. At the second level, the measured performance of the SDHW is compared to the results of a simulation model on a daily basis.

The feasibility of the proposed method is assessed by performing a retrospective analysis using three years of monitoring data from a real SDHW system located in Montréal, Canada.

The rule-based algorithm identified most of the major system faults (e.g. auxiliary heater failure) and instrumentation errors (e.g. disconnected sensor). In an online monitoring context, these faults would have been detected within a short time interval (e.g. 15 minutes).

The daily simulation-based AFD was able to identify performance related faults that were not always clearly

identified by the rule-based algorithm. These faults were mostly related to a badly positioned collector outlet temperature sensor or too low antifreeze concentration in the solar loop.

Using rule-based and simulations-based methods for AFD combines the detection capabilities of both methods, and has the potential to reduce the number of false alarms that can lead to AFD systems being ignored or disabled. It can give key information to help diagnose the cause of the detected faults. It can contribute to increasing the reliability of SDHW systems if it is integrated into an effective user interface.

7. References

de Keizer, Ae.C., Kuethe, S., Jordan, U., Vajen, K., 2013. Simulation-based long-term fault detection for solar thermal systems. Sol. Energy 93, 109–120.

de Keizer, A.C., Vajen, K., Jordan, U., 2011. Review of long-term fault detection approaches in solar thermal systems. Sol. Energy 85, 1430–1439.

He, H., Caudell, T.P., Menicucci, D.F., Mammoli, A. a., 2012. Application of Adaptive Resonance Theory neural networks to monitor solar hot water systems and detect existing or developing faults. Sol. Energy 86, 2318–2333.

Holter, C., Gerardts, B., Ohnewein, P., Dröscher, A., Feichtner, F., Schgaguler, K., Meißner, E., Luidolt, P., Köstinger, A., Heimrath, R., Streicher, W., 2011. IP-Solar: Development and validation of a web-based monitoring and diagnostics tool for solar thermal systems, in: Proceedings of the 30th ISES Biennial Solar World Congress 2011. Elsevier B.V., Kassel, Germany, pp. 4467–4475.

Kalogirou, S., Lalot, S., Florides, G., Desmet, B., 2008. Development of a neural network-based fault diagnostic system for solar thermal applications. Sol. Energy 82, 164–172.

Klein, S. A., Beckman, W. A., Mitchell, J. W., Duffie, J. A., Duffie, N. A., Freeman, T. L., Mitchell, J. C., Braun, J. E., Evans, B. L., Kummer, J. P., Urban, R. E., Fiksel, A., Thornton, J. W., Blair, N. J., Williams, P. M., Bradley, D. E., McDowell, T. P., Kummert, M. and Duffy, M. J. (2014) 'TRNSYS 17 – A TRaNsient SYstem Simulation program, User manual. Version 17.2'. Madison, WI: University of Wisconsin-Madison.

Küthe, S., de Keizer, A.C., Shahbazfar, R., Vajen, K., 2011. Implementation of data processing and automated algorithm based fault detection for solar thermal systems, in: Proceedings of the 30th ISES Biennial Solar World Congress 2011. Kassel, Germany, pp. 4443–4450.

Maltais Larouche, S., 2016. Détection de faute automatique dans les systèmes solaires thermiques basée sur la vérification de règles et la simulation. Master of Applied Science thesis, Polytechnique Montréal, QC, CAN.

Menicucci, D., 2009. Assembly and Comparison of Available Solar Hot Water System Reliability Databases and Information. Sandia National Laboratories, Albuquerque, New Mexico and Livermore, California.

Pärisch, P., Vanoli, K., 2007. Quality assurance of solar thermal systems with the ISFH- Input / Output-Procedure, in: Proceedings of the 3rd European Thermal Energy Conference. Freiburg, Germany, pp. 315–320.

Thornton, J.W., Blair, N.J., Naik, A.V., Bradley, D.., Duffy, M.J., McDowell, T.P., LaHam, N.D., 2013. TESSLibs 17 - Component Libraries for the TRNSYS Simulation Environment. Thermal Energy System Specialists, Madison, WI.

Viessmann, 2015. Vitosol System Design Guide. Viessmann Manufacturing Company Inc., Waterloo, ON, Canada.

Yaïci, W., Entchev, E., 2014. Performance prediction of a solar thermal energy system using artificial neural networks. Appl. Therm. Eng. 73, 1348–1359.